

---

**ARTICLE**

---

**Activation benchmark study at a 2.5 GeV electron accelerator**

Markus Brugger<sup>a</sup>, Abderrahim Errahhaoui<sup>a</sup>, Minho Kim<sup>b</sup>, Hee-Seock Lee<sup>b</sup>, Stefan Roesler<sup>a\*</sup> and Heinz Vincke<sup>a</sup>

<sup>a</sup>CERN, CH-1211 Geneva 23, Switzerland; <sup>b</sup>Pohang Accelerator Laboratory / POSTECH, Pohang, 790-784, Korea

Samples of copper, aluminium and stainless steel with well-characterized elemental compositions were irradiated in the stray radiation field created by a 2.5 GeV electron beam hitting a copper dump. After the irradiation the induced activity in the samples was analysed with gamma-ray spectrometry. The beam intensity monitoring with a current transformer was verified in an additional study by irradiating gold-foils stacked in between copper blocks and by analysing the production of <sup>196</sup>Au for which detailed experimental cross section data exist. All results were finally compared to the predictions obtained with the FLUKA Monte-Carlo code. Excellent agreement between measurement and simulation within a few percent was obtained for the gold-foils irradiation confirming the accuracy of the beam monitoring. The benchmark of the FLUKA results with the data of the material samples showed good agreement, for many nuclides within 30%.

**Keywords:** Activation; Monte Carlo; FLUKA; high-energy electron accelerator

**1. Introduction**

Accurate predictions of induced radioactivity is essential for the design, operation and decommissioning of high energy electron facilities. While Monte Carlo predictions of activation around high-energy hadron accelerators have been extensively benchmarked in the past, much less experimental information is available from high-energy electron accelerators. The present study addresses this lack of data with an experiment performed at the Pohang Accelerator Laboratory (PAL) in South Korea.

Its setup and methods resemble those of a previous experiment [1]. Materials typically used at accelerators were exposed to the stray radiation field created by a 2.5 GeV electron beam hitting a copper dump. After the irradiation the induced activity in the samples was analysed with gamma-ray spectrometry. The beam intensity monitoring was verified by irradiating gold-foils stacked in between copper blocks and by analysing the production of <sup>196</sup>Au for which detailed experimental cross section data exist.

The irradiation experiment was also simulated with the Monte Carlo particle transport code FLUKA [2,3] and results were compared with the measured data.

**2. Irradiation experiment**

The cylindrical copper dump, 25.4 cm in length and 5.08 cm in radius, was placed inside of a shielded area located at the downstream end of the PAL linear

accelerator that supplies the synchrotron facility with electrons at 2.5-GeV energy. Switching magnets allowed steering the beam either towards the storage ring for filling it about twice per day or onto our copper dump during the remaining time.

Cylindrical samples of copper, aluminium and stainless steel with well-characterized elemental compositions (see **Table 1**) were placed around the target at nine well-defined positions using an aluminium holder. The setup is shown in **Figure 1**. A copper and an aluminium sample were placed at each of the three sample positions on top of the dump (labelled “T1-3”) in order to investigate the activation along the shower axis. The holder-“cups” to the left and right of the dump at a certain longitudinal position (labelled “L”) contained samples of the same material to check uncertainties in the beam alignment: aluminium (diameter: 1.2 cm, thickness: 1.2 cm) in the most upstream cups, steel (diameter: 0.5 cm, thickness: 1.0 cm) in the centre ones and copper (diameter: 1.3 cm, thickness: 0.6 cm) in the most downstream cups. In addition to these lateral sample positions, one sample of each material (diameter: 2 cm, thickness 0.6 cm) was also placed downstream of the dump aligned with the beam axis (see Figure 1).

The irradiation took three days and 21 hours during which  $1.1 \times 10^{16}$  electrons were sent onto the dump with an average power of 16 W. An integrating current transformer provided the beam intensity monitoring at a frequency of 2 Hz, complemented by an independent counting of beam pulses. The beam intensity monitoring was verified in a separate activation study using gold foils (not shown here) and found to be accurate to within a few percent. The beam spot could be observed from

---

\*Corresponding author. Email: Stefan.Roesler@cern.ch

the laboratory throughout the entire irradiation using a camera and a fluorescence screen attached to the front face of the dump.

The samples were taken out in three batches in order to measure the induced activity of short-lived nuclides with gamma-ray spectrometry in preparation of their shipping to CERN for a more detail analysis.

Table 1. Elemental composition of the samples [1].

	Steel	Copper	Aluminium
Fe	63.088	Cu	99.328
Cr	17.79	Al	0.4745
Mn	11.43	Si	0.13
Ni	6.5	Fe	0.0261
Si	0.38	S	0.0137
N	0.31	Cd	0.004
Co	0.11	Sb	0.004
P	0.019	Cr	0.0021
C	0.095	Te	0.002
Mo	0.09	Pb	0.002
Cu	0.085	Sn	0.002
V	0.07	As	0.002
Ti	0.01	Ag	0.002
Nb	0.01	Zn	0.002
W	0.01	Mn	0.0016
O	0.002	Se	0.0011
S	0.001	Bi	0.001
		Ni	0.001
		P	0.0004
		Co	0.0002
		Zr	0.0024

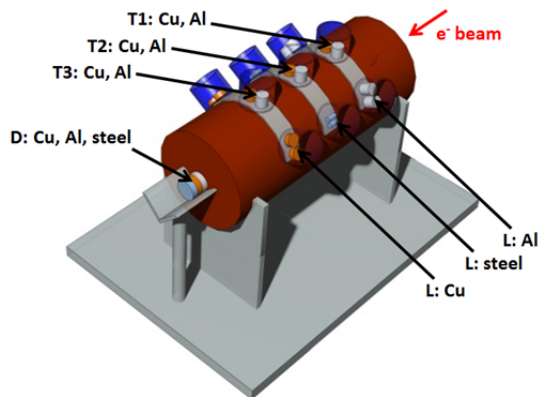


Figure 1. FLUKA geometry of the irradiation setup visualized with SimpleGeo [4]. The beam hits the copper target in the center of the circular surface from the top right side. The samples are labeled with 'L' for lateral side, 'T1-3' for lateral top and 'D' for downstream positions.

After arrival at CERN detailed gamma-ray spectrometry measurements were performed on all samples using a low-background coaxial high precision Germanium detector. In order to explore nuclides with intermediate and long half-lives each sample was measured twice, 10-18 days and 4-5 months after the irradiation, respectively. For nuclides that were identified in both measurements, only the data point with the lower uncertainty was retained for the

comparison with the FLUKA prediction, taking also into account its ratio to the Minimum Detectable Activity (MDA). Data with ratios below one were excluded from the comparison.

### 3. FLUKA calculations

The activation data of the samples were used to benchmark FLUKA2011 Version 2.4 [2,3]. Beside the precise geometry modeling of the irradiation setup (see Figure 1) the most accurate models for activation studies were selected: the evaporation of fragments with masses up to  $A=24$ , coalescence effects in the emission of nucleons as well as the PEANUT nuclear model for interactions at all energies.

The beam was assumed to be centered on the dump front face and its direction aligned with the dump axis. The beam spot was defined with a Gaussian distribution in vertical direction ( $\sigma=1.1$  mm) and with a rectangular distribution in horizontal direction (total width of 7 mm). Transport thresholds were set at 10 MeV for electrons and positrons and 5 MeV for photons, respectively (*i.e.*, above the photo-production threshold for all materials). All hadrons were followed in energy until stopped or captured, including thermal neutrons. The results reported below represent averages over  $4 \times 10^8$  primary electrons. The predicted nuclide inventories in the samples were processed offline for radioactive built-up and decay taking into account in detail the measured time profile and intensity of the beam.

Figure 2 shows energy fluence spectra of secondary neutrons and photons at the downstream and lateral sample locations normalized per primary electron.

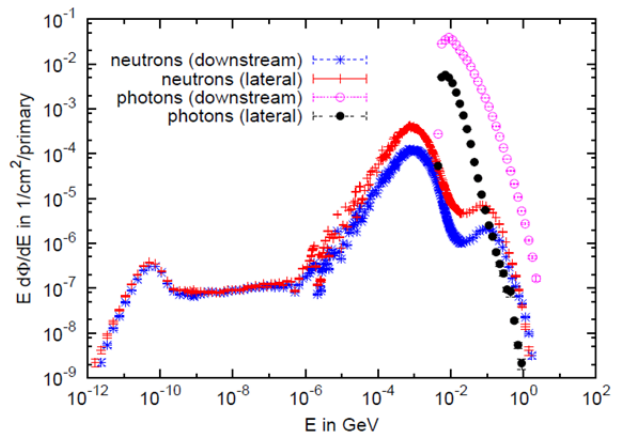


Figure 2. Energy fluence spectra of neutrons and photons at the downstream and lateral irradiation positions.

The spectra clearly indicate that activation is dominated by neutron interactions at the lateral sample positions and by photo-production processes downstream of the dump. At the latter locations the photon fluence above a few MeV in energy exceeds that of neutrons by orders of magnitude, over-compensating the generally lower hadronic cross sections of photons.

### 4. Results and discussion

Tables 2-4 show the measured specific activities in the samples downstream of the dump. The activity values refer to the time of the start of the respective gamma-ray measurement. Nuclides with half-lives below that of <sup>46</sup>Sc (83.8d) were measured at cooling times of 10-18 days, nuclides with longer half-lives at cooling times between 4-5 months, respectively. The tables also give for each nuclide the ratio of measured activity and MDA that provides an additional indication of the reliability of the experimental result. Finally, the last column shows the ratios of FLUKA predictions and measured activities. For the latter, the quoted errors are obtained as sum of the relative uncertainties of the measurement and of the calculated values (considering only statistical errors).

Table 2. Specific activities of nuclides measured in the downstream stainless steel sample. The last but one column shows the ratios of the measured activities (labeled 'M') and the MDA values. The last column shows the ratios of FLUKA predictions and measured activities. Uncertainties in percent are given in parentheses.

Isotope	<i>t</i> <sub>1/2</sub>	Measurement (Bq/g)	ratio M/MDA	ratio FLUKA/M
<sup>46</sup> Sc	83.8d	0.31 (7.0%)	25	0.83 (8.8%)
<sup>48</sup> V	16.0d	8.8 (5.9%)	220	1.9 (6.7%)
<sup>51</sup> Cr	27.7d	1030. (11%)	1515	1.2 (12%)
<sup>52</sup> Mn	5.6d	3.7 (5.8%)	89	2.2 (6.4%)
<sup>54</sup> Mn	312.1d	42. (8.2%)	2600	0.62 (8.4%)
<sup>59</sup> Fe	44.5d	0.10 (33%)	1.6	0.41 (40%)
<sup>56</sup> Co	77.3d	3.2 (5.2%)	263	1.25 (5.8%)
<sup>57</sup> Co	271.79d	55. (9.8%)	1957	0.93 (9.9%)
<sup>58</sup> Co	70.82d	19. (8.2%)	326	0.76 (8.6%)
<sup>57</sup> Ni	35.6h	0.24 (16%)	5.0	0.46 (17%)

Table 3. As in Table 2, here for the downstream Al sample.

Isotope	<i>t</i> <sub>1/2</sub>	Measurement (Bq/g)	ratio M/MDA	ratio FLUKA/M
<sup>22</sup> Na	2.6y	1.6 (7.8%)	188	1.1 (8.6%)
<sup>46</sup> Sc	83.8d	0.076 (17%)	2.8	0.54 (29%)
<sup>48</sup> V	16.0d	0.12 (15%)	4.5	1.1 (32%)
<sup>51</sup> Cr	27.7d	11. (12%)	31	0.34 (15%)
<sup>52</sup> Mn	5.6d	0.11 (14%)	5.0	1.7 (21%)
<sup>54</sup> Mn	312.1d	6.5 (8.2%)	587	1.1 (8.8%)
<sup>57</sup> Co	271.79d	0.032 (20%)	4.2	4.0 (26%)
<sup>58</sup> Co	70.82d	0.041 (43%)	1.6	3.0 (51%)
<sup>65</sup> Zn	244.26d	0.12 (24%)	6.8	3.3 (27%)

Taking the uncertainties into account the FLUKA predictions agree with the experimental data within 30% for many nuclides in the copper and stainless steel samples. Furthermore, the ratios scatter around one, indicating no systematic over- or underestimation by FLUKA. The nuclides identified in the aluminium sample (Table 3) result mostly from reactions on trace elements and, thus, carry the uncertainty of the elemental composition. Nuclides produced on trace

elements can be relevant in the characterization of radioactive waste and this study indicates the uncertainties that have to be considered in this case. The only nuclide produced directly in interactions on aluminium nuclei (<sup>22</sup>Na) is well reproduced by FLUKA.

Table 4. As in Table 2, here for the downstream Cu sample.

Isotope	<i>t</i> <sub>1/2</sub>	Measurement (Bq/g)	ratio M/MDA	ratio FLUKA/M
<sup>46</sup> Sc	83.8d	0.031 (11%)	4.6	0.68 (17%)
<sup>48</sup> V	16.0d	0.46 (7.6%)	27.1	1.1 (12%)
<sup>51</sup> Cr	27.7d	2.3 (16%)	6.5	0.73 (18%)
<sup>52</sup> Mn	5.6d	0.40 (6.7%)	24.9	0.68 (10%)
<sup>54</sup> Mn	312.1d	0.51 (8.4%)	60.7	0.73 (9.9%)
<sup>59</sup> Fe	44.5d	0.93 (8.8%)	25.3	0.32 (13%)
<sup>56</sup> Co	77.3d	1.2 (5.8%)	55.5	1.2 (7.5%)
<sup>57</sup> Co	271.79d	2.4 (9.9%)	257.	0.82 (11%)
<sup>58</sup> Co	70.82d	31.9 (7.4%)	1181.	2.1 (7.6%)
<sup>60</sup> Co	5.27y	0.53 (6.4%)	92.8	0.65 (6.9%)
<sup>65</sup> Zn	244.26d	0.079 (11%)	7.2	0.37 (17%)

As mentioned earlier, photo-production processes dominate the production of nuclides in the downstream samples. Thus, the results can be considered as direct verification of the implementation of these interactions in FLUKA.

It should be noted that the production of <sup>59</sup>Fe in stainless steel (by thermal neutron capture on <sup>58</sup>Fe) is underestimated by about a factor of two due to the fact that the simulations did not include the rather complex concrete enclosure around the experimental setup and, thus, underestimate the thermal neutron fluence. However, <sup>59</sup>Fe is the only nuclide in the presented results that is sensitive to the thermal neutron fluence justifying this geometry approximation.

Tables 5-7 show the results for the samples at the lateral irradiation positions. As mentioned above, several samples of each material were placed, e.g., a copper and an aluminium sample in each of the top positions and samples of the same material on either side of the dump. Thus, for a certain nuclide up to four results are reported in the tables. The last column indicates the exact location: "T" refers to a lateral top position and "L" to a lateral side position (see also Figure 1).

Table 5. As in Table 2, here for the aluminium samples in lateral side and top positions. The last column indicates the position of the sample.

Isotope	<i>t</i> <sub>1/2</sub>	Measurement (Bq/g)	ratio M/MDA	ratio FLUKA/M	pos.
<sup>22</sup> Na	2.6y	0.68 (8.6%)	48	0.65 (11%)	L
		0.70 (8.9%)	43	0.62 (11%)	T1
		0.45 (9.8%)	25	0.74 (12%)	T2
		0.28 (13.5%)	13	0.81 (17%)	T3

Table 6. As in Table 2, here for the copper samples in lateral side and top positions.

Isotope	$t_{1/2}$	Measurement		ratio		pos.	
		(Bq/g)		M/MDA	FLUKA/M		
<sup>46</sup> Sc	83.8d	0.052	(13%)	3.7	0.90	(21%)	T1
		0.10	(19%)	2.9	0.77	(29%)	T2
		0.048	(25%)	2.4	0.80	(38%)	T3
		0.043	(25%)	2.4	0.93	(38%)	L
<sup>47</sup> Sc	80.28h	0.18	(22%)	3.6	0.80	(36%)	T1
<sup>48</sup> V	16.0d	0.80	(7.4%)	25	1.3	(15%)	T1
		0.59	(7.9%)	21	1.3	(16%)	T2
		0.29	(8.8%)	15	1.3	(19%)	T3
		0.24	(9.4%)	12	1.1	(20%)	L
<sup>51</sup> Cr	27.7d	3.5	(15%)	7.1	0.69	(19%)	T1
		2.2	(17%)	5.6	0.78	(22%)	T2
		1.0	(20%)	4.4	0.93	(26%)	T3
		0.89	(24%)	3.3	0.88	(30%)	L
<sup>52</sup> Mn	5.6d	1.4	(6.3%)	42	0.61	(12%)	T1
		0.84	(6.6%)	32	0.76	(13%)	T2
		0.42	(7.3%)	23	0.79	(16%)	T3
		0.29	(8.0%)	17	0.72	(17%)	L
<sup>54</sup> Mn	312.1d	0.77	(8.6%)	48	0.62	(11%)	T1
		0.42	(8.9%)	35	0.74	(12%)	T2
		0.18	(10%)	20	0.82	(15%)	T3
		0.14	(11%)	15	0.89	(16%)	L
<sup>59</sup> Fe	44.50d	1.9	(8.9%)	27	0.32	(16%)	T1
		1.1	(9.4%)	17	0.37	(18%)	T2
		0.50	(11%)	12	0.34	(22%)	T3
		0.36	(11%)	9.4	0.45	(23%)	L
<sup>56</sup> Co	77.3d	0.49	(6.5%)	33	1.2	(9.8%)	T1
		0.80	(7.1%)	22	1.3	(11%)	T2
		0.38	(8.4%)	15	1.5	(14%)	T3
		0.32	(9.0%)	13	1.1	(15%)	L
<sup>57</sup> Co	271.79d	2.3	(10%)	113	0.72	(12%)	T1
		1.2	(10%)	107	0.87	(12%)	T2
		0.53	(11%)	54	1.0	(13%)	T3
		0.41	(11%)	41	1.1	(14%)	L
<sup>58</sup> Co	70.82d	18.	(8.1%)	354	0.69	(9.0%)	T1
		11.	(8.2%)	287	0.96	(9.1%)	T2
		5.6	(8.3%)	209	1.3	(9.4%)	T3
		4.4	(8.4%)	164	1.3	(9.4%)	L
<sup>60</sup> Co	5.27y	0.86	(6.5%)	72	0.38	(7.4%)	T1
		0.53	(6.7%)	58	0.38	(7.8%)	T2
		0.22	(7.4%)	28	0.45	(9.2%)	T3
		0.18	(7.7%)	27	0.44	(9.4%)	L
<sup>65</sup> Zn	244.26d	0.052	(18%)	2.2	0.39	(34%)	T1
		0.038	(36%)	2.0	0.35	(53%)	T2
		0.013	(35%)	1.2	0.45	(62%)	T3

Laterally to the dump the nuclide production in the samples is dominated by interactions of secondary neutrons produced by photo-production processes inside the dump. Along the top of the dump the ratios of FLUKA predictions and experimental data tend to increase (e.g., <sup>51</sup>Cr in Table 6, see Figure 1 for the sample positions), probably pointing to slight discrepancies between simulated and actual longitudinal shower development inside the dump.

It should be noted that FLUKA does not predict the production of meta-stable states. Instead, equal sharing of the cross section is assumed between meta-stable and

ground states. This could partially explain, e.g., the results for <sup>44m</sup>Sc/<sup>44</sup>Sc in the stainless steel sample (see Table 7).

Table 7. As in Table 2, here for a lateral stainless steel sample.

Isotope	$t_{1/2}$	Measurement		ratio	
		(Bq/g)		M/MDA	FLUKA/M
<sup>44</sup> Sc	3.9h	0.38	(25%)	3.2	1.1 (33%)
<sup>44m</sup> Sc	58.6h	0.65	(22%)	3.6	0.62 (30%)
<sup>46</sup> Sc	83.8d	0.29	(10%)	9.9	0.84 (16%)
<sup>48</sup> V	16.0d	7.4	(6.5%)	57	1.2 (11%)
<sup>51</sup> Cr	27.7d	202.	(11%)	126	1.1 (12%)
<sup>52</sup> Mn	5.6d	7.7	(6.0%)	64	1.1 (10%)
<sup>54</sup> Mn	312.1d	11.8	(8.3%)	337	0.61 (9.5%)
<sup>56</sup> Co	77.3d	2.0	(8.3%)	15	1.1 (14%)
<sup>57</sup> Co	271.79d	7.2	(10%)	168	1.0 (11%)
<sup>60</sup> Co	5.27y	0.11	(15%)	4.5	0.39 (19%)
<sup>57</sup> Ni	35.6h	1.7	(11%)	12	0.53 (15%)

## 5. Conclusion

The present study provides a large amount of experimental activation data for high-energy electron accelerators that can be used to benchmark Monte Carlo codes. Emphasis was put on the activation of copper, stainless steel and aluminium, materials widely used for accelerator construction. The irradiation setup was simulated in detail with the FLUKA Monte Carlo code. The measured and predicted specific activities show good agreement within 30% for many nuclides.

## References

- [1] J. Bauer, V. Bharadwaj, H. Brogonia, M. Brugger, M. Kerimbaev, J.C. Liu, S. Mallows, A.A. Prinz, S. Roesler, S. Rokni, T. Sanami, M. Santana-Leitner, J. Sheppard, H. Vincke and J. Vollaie, Benchmark study of induced radioactivity at a high energy electron accelerator, Part I: Specific activities, *Proc. 1<sup>st</sup> ARIA Workshop*, PSI, Switzerland, Oct. 13-17, 2008, (2008), pp. 96-106.
- [2] A. Fassò, A. Ferrari, J. Ranft and P.R. Sala, *FLUKA: A Multi-Particle Transport Code*, CERN-2005-10, INFN/TC\_05/11 (2005).
- [3] G. Battistoni, S. Muraro, P.R. Sala, F. Cerutti, A. Ferrari, S. Roesler, A. Fassò and J. Ranft, The FLUKA code: Description and benchmarking, *Proc. Hadronic Shower Simulation Workshop 2006*, Fermilab, Sept. 6-8, 2006, M. Albrow, R. Raja eds., AIP Conf. Proceedings 896, (2007), pp. 31-49.
- [4] C. Theis, K.H. Buchegger, M. Brugger, D. Forkel-Wirth, S. Roesler and H. Vincke, Interactive three dimensional visualization and creation of geometries for Monte Carlo calculations, *Nucl. Instr. and Meth. A* 562 (2006), pp.827-829.